

# A novel AC excited axial flux synchronous motor for electric vehicles

N. A. El - Sonbaty

Electrical Eng. Dept., Faculty of Eng., Zagazig University, Egypt

The paper presents a novel AC excited self-started Axial Flux Synchronous Motor (AFSM) with a view to fulfill the special requirements for Electric Vehicles (EVs) in their optimum profiles.. The motor has a single double-sided slotted wound rotor sandwiched between twin stator. All three cores are of disc type. Electrical equivalent circuit of the AFSM is proposed. Theory of operation, performance analysis and simulation results for the motor are given. Test results validate the optimum performance of the new proposed EV motor drive.

يقدم البحث محرك جديد ثلاثي الأوجه محوري الفيض يحقق المتطلبات الخاصة والمرجوة من محرك المركبة الكهربائية. يتكون المحرك من عضوين ثابتين توأمين كل منهما على شكل قرص به مجاري تحتوي على ملفات ثلاثية الأوجه - يوصل كل وجه بنظيره في العضو الثابت الأخر على التوالي. ويدور بين هذين القرصين قرص ثالث يمثل العضو الدائر ويحتوي على مجاري على كلا الجانبين ، بكل منهما ملفات ثلاثية الأوجه ويوصل كل وجه بالتوالي العكسي مع نظيره بحيث تكون ق . د . ك . المستنتجة بالتأثير في أحدهما متضادة مع نظيرتها في الملف الآخر وذلك لملاشاة العزوم التأثيرية لتصبح العزوم كلها تزامنية فقط . يعطي المحرك خواص مشابهة لمحرك التوالي حيث يعمل المحرك مباشرة في نطاق القدرة الثابتة ( دون التشغيل في منطقة ثبوت العزم ) . ويتم ربط المحرك مباشرة بين عجلتي المركبة دون الاستعانة بصندوق التروس والوسائط الميكانيكية لفصل الحركة وتوصيلها ، ويمتاز بأن سرعة تشغيله القسوى تتساوى مع السرعة القسوى للمركبة الكهربائية . ويشتمل البحث أيضاً على النقاط التالية: ١ - استنتاج نظرية التشغيل للمحرك المقترح. ٢ - تحليل أداء المحرك والحصول على خصائصه. ٣ - تحقيق الفكرة الأساسية للبحث معملياً والحصول على الخصائص المثالية المطلوبة لمحرك المركبة الكهربائية .

**Keywords:** Electric vehicles, Electric traction, Synchronous motors, Electric Drives, Axial flux machines

## 1. Introduction

The two most important characteristics needed for the Electrical Vehicles (EV) and Hybrid Electric Vehicle (HEV) motor drives are the wide speed constant power capability and the high operating efficiency. Modern electric motors have benefited from design and material innovations. Availability of low loss, high grade, stress relieved, coated electrical steel laminations have contributed significantly to the improvement of efficiency and reduction in size of modern electric motors. Extended constant power capability, on the other hand, is dependent on the motor type, its design, and the control strategy. DC commutator motors are inherently suited for extended constant power operation. However, commutation problems, low maximum speed capability, poor efficiency and bulky nature limit their operation in vehicle applications [1]. Break down torque in induction motors limits

their extended speed constant power capability due to the natural torque speed curve ( $Ta 1/n^2$ ) at constant stator voltage not fitting the special condition encountered in vehicle drive ( $Ta 1/n$ ). The non-linearity of its dynamic model makes the control complex. Moreover, induction motors have an inherent disadvantage of slip-dependent rotor copper loss, and there is the problem of heat extraction from the machine core [2]. Permanent magnet synchronous motors have several distinct advantages namely, high efficiency, high power factor and smooth brushless operation [3]. The present cost of high-energy rare earth magnets (*ND-FE-B*) are quite high. Magnet corrosion and relatively temperature tolerance are potential hazards. Furthermore, fixed flux level results in very limited constant power speed range. Therefore, PM with hybrid excitation combination has been recently developed [4]. In recent years, axial-flux machines and new discoidal topologies are becoming prime

movers in electric vehicle propulsion systems, principally as wheel – direct coupling motors so the mechanical differential and transmission systems can be eliminated. More over, for electric vehicles the weight reduction is a mandatory requirement due to the direct impact on electric energy consumption that affects seriously the vehicle autonomy. Axial flux machines using permanent magnet allow machine design with improved performance, but still remain more expensive. Furthermore, these machines are also less flexible in the flux control mode leading to a complex design of the control system and present some problems, like thermal and mechanical stability [5, 6]. In this investigation to explore the features of robustness, high power and torque density, high efficiency and optimum torque speed characteristics, a new axial synchronous motor is proposed.

## 2. EV motor considerations

The following technologies are cited for choosing the proper electric vehicle motor drives.

### 2.1. Direct wheel motor drive

Several advantages as elimination of transmission and gearing losses, better power train, fault tolerance improvements, fewer suspension struts requirements and reduced height for multi-wheel vehicles will be achieved with direct wheel motor drive [7, 8]. During a driving cycle, the required wheel torque is:

$$T_w = F_{tr} r. \quad (1)$$

The motor rotational speed  $n$  (rpm) is related to the vehicle speed  $v$  ( $km/h$ ) by:

$$n = 1000 v i / (120 \pi r). \quad (2)$$

Where  $F_{tr}$  is the tractive force,  $r$  is the wheel radius (m) and  $i$  is the gear ratio.

For direct drive and aiming to elimination of the reduction gearbox, the motor maximum speed must correspond to the vehicle maximum speed. Thus for electric vehicle

maximum speed of 160 km/h [9, 10], the corresponding maximum motor speed is about 1500 rpm for wheel radius of 0.2794 m (11 inch).

### 2.2. Axial flux motor

It has been concluded by refs. [5, 6, 11-14] that the Axial Flux (AF) configuration has substantial advantages over the conventional Radial Flux (RF) machines. It presents a better power density ratio, which increases as the number of poles increases. Thus the axial flux machine have the desired advantages of high torque at low speeds for hill climbing and low torque at high speeds for cruising. Axial flux motors have a relatively higher starting torque and higher efficiency due to less stator resistance. The maximum torque is slightly lower than that of the radial flux due to the slightly higher stator leakage reactance. Steady state performances and parameters comparison is given in refs. [13-14]. Axial flux machines have suitable shape to match the space constraints and they are almost maintenance free.

### 2.3. Minimum power requirement

Ref. [1] has concluded that the power requirement is minimum when the motor operation is entirely in the constant power region. Thus motors with high pole numbers seemed to be attractive for EV due to its low rated speed.

### 2.4. Optimal torque – speed profile for EV

The study for optimal torque – speed profile given in ref. [1] reveals that (i) the extended constant power operating range (of 4 -6 times base speed) is important for both initial acceleration and cruising intervals of operation (ii) The optimum torque ( $T$ ) –speed ( $n$ ) profile is  $T \propto 1/n$  when entirely operating within the constant power region. The main advantage of the proposed motor is the constant power range operation in the range of base speed, with small number of poles (4 pole). This leads to high specific power of the motor with higher efficiency.

### 3. Machine description

Taking the above considerations into account, the proposed motor has been chosen to be 3-phase, 4 pole direct wheel drive with axial flux, single double- sided slotted wound rotor sandwiched between twin stator. The three cores are of disc type with slots to allocate the stators and rotor windings. The rotor core with slots on both radial sides in which two identical three phase windings are connected in such a way that the rotor current supplied from the inverter flows in reverse directions in each of the two back - to - back rotor slots, to eliminate the induction *e. m .f.* from rotor to stator and vice versa. The twin stator windings are in same polarity series connection (the current flow in the same direction in any two back - to back stator slots) and fed from 50 Hz, bus bar. Schematic of the proposed structure is shown in fig.1. The motor will be self started when the rotor frequency is set to be equal to the stator frequency provided that the two resulted rotating fields are of opposite directions (stationary rotor). Then, by gradually decreasing of rotor frequency, the motor speed will be increased.

### 4. Mathematical model

First the machine is represented by the equivalent circuit shown in fig. 2.  $V_s$  is the 50 Hz supply voltage applied to the stator (twin stators) and  $V_r$  is the variable frequency Voltage applied to the rotor (twin rotors). As a doubly fed induction motor but with a special connection (reverse series rotor windings connection), the following voltage equations are deduced, using super position theorem. Eqs. (3, 4) represent stator fed system with short circuited rotor (through the frequency converter), while eqs. (5, 6) represent rotor fed system with short circuited stator (through the supply):

$$V_s = I_{s1}[(r_{sa} + r_{sb}) + j\omega_1(L_{sa} + L_{sb})] + j\omega_1 L_{msa} I_{r1} e^{-j\delta} + j\omega_1 L_{msb} I_{r1} e^{j(\pi-\delta)}, \quad (3)$$

$$0 = I_{r1}[(r_{ra} + r_{rb}) + j\omega_2(L_{ra} + L_{rb})] + j\omega_2 L_{mra} I_{s1} e^{j\delta} + j\omega_2 L_{mrb} I_{s1} e^{j(\pi-\delta)}, \quad (4)$$

$$V_r = I_{r2}[(r_{ra} + r_{rb}) + j\omega_2(L_{ra} + L_{rb})] + j\omega_2 L_{mra} I_{s2} e^{j\delta} + j\omega_2 L_{mrb} I_{s2} e^{j(\pi-\delta)}, \quad (5)$$

and

$$0 = I_{s2}[(r_{sa} + r_{sb}) + j\omega_1(L_{sa} + L_{sb})] + j\omega_1 L_{msa} I_{r2} e^{-j\delta} + j\omega_1 L_{msb} I_{r2} e^{-j(\pi-\delta)}. \quad (6)$$

Combining eq. (3) with eq. (6) and eq. (4) with eq. (5) and simplifying, gives the two following voltage equations from which the equivalent circuit of fig. 3 is deduced.

$$V_s = I_s (r_{sa} + r_{sb}) + j\omega_1 I_s (L_{sa} + L_{sb}) + E_{rs}, \quad (7)$$

$$K_c V_s = I_r (r_{ra} + r_{rb}) + j\omega_2 I_r (L_{ra} + L_{rb}) + E_{sr}. \quad (8)$$

Where:

$$\bar{I}_s = \bar{I}_{s1} + \bar{I}_{s2}, \quad \bar{I}_r = \bar{I}_{r1} + \bar{I}_{r2},$$

$$E_{rs} = -j\omega_1 L_{ms} I_r \cos \delta,$$

$$E_{sr} = j\omega_2 L_{mr} I_s \cos \delta,$$

and

$$K_c = \omega_2 a / \omega_1.$$

Where *a* is the stator/rotor transformation ratio . The stator and rotor inductance's are;

$$\begin{aligned} L_{sa} &= L_{sla} + L_{msa}, \\ L_{sb} &= L_{slb} + L_{msb}, \\ L_{ms} &= L_{msa} + L_{msb}, \\ L_{ra} &= L_{rla} + L_{mra}, \\ L_{rb} &= L_{rlb} + L_{mrb} \text{ and} \\ L_{mr} &= L_{mra} + L_{mrb}. \end{aligned}$$

Since the machine is twin stator and twin rotor, the above equations are solved in terms of one stator part and one rotor part, say *a*. The stator current  $I_s$  and the rotor current  $I_r$  will be:

$$I_s = 0.5 V_s [ (r_{ra} - K_c \omega_1 L_{ms} \sin \delta) + j\omega_2 L_{ra} ] / \{ [r_{sa} r_{ra} \omega_1 \omega_2 (L_{sa} L_{ra} - L_{ms}^2 \sin^2 \delta)] + j(\omega_1 L_{sa} r_{ra} + \omega_2 L_{ra} r_{sa}) \}, \quad (9)$$

$$I_r = 0.5 V_s [ (K_c r_{sa} + \omega_2 L_{ms} \sin \delta) + j K_c \omega_1 L_{sa} ] / \{ [r_{sa} r_{ra} \omega_1 \omega_2 (L_{sa} L_{ra} - L_{ms}^2 \sin^2 \delta)] + j(\omega_1 L_{sa} r_{ra} + \omega_2 L_{ra} r_{sa}) \}. \quad (10)$$

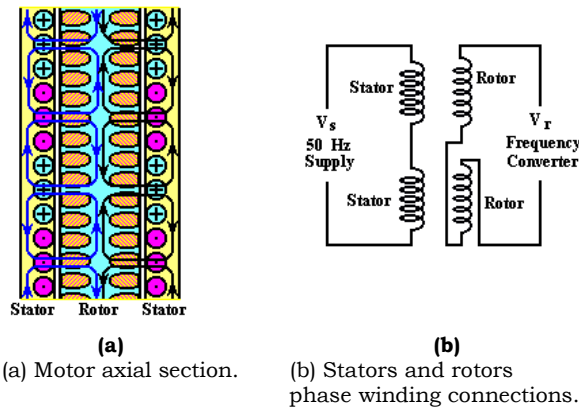


Fig. 1. Proposed AFSM motor.

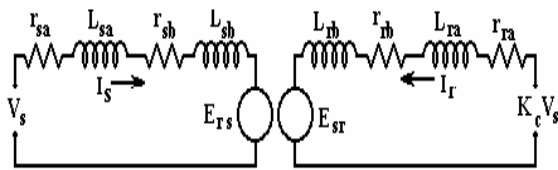


Fig. 2. Detailed equivalent circuit per phase

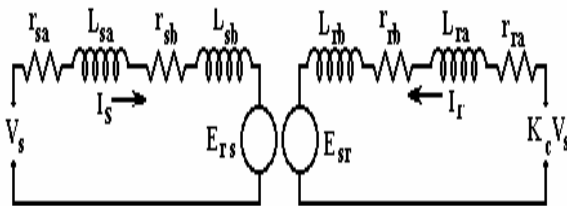


Fig. 3. Per phase equivalent circuit.

The Total mechanical power  $P_m$  is;

$$P_m = 3 (2p) [Re \{ E_{sr} I_r^* \} + Re \{ E_{rs} I_s^* \}]. \quad (11)$$

The output power  $P_o$  is;

$$P_o = P_m - P_{fw}.$$

And the motor torque  $T$  is;

$$T = P_o / \omega_m. \quad (12)$$

Where;

$$\omega_m = \omega_1 \pm \omega_2. \quad (13)$$

The rotor speed  $N_r$  is;

$$N_r = 120(f_s \pm f_r) / (2p). \quad (14)$$

The input power  $P_{in}$  is;

$$P_{in} = 3 V_s [I_s \cos \phi_s + K_c I_r \cos \phi_r]. \quad (15)$$

The stator iron loss and the rotor iron loss are given by:

$$P_{irs} = 3(\omega_1 L_{ms} I_{r1} \sin \delta)^2 / R_{ms}, \quad (16)$$

and

$$P_{irr} = 3(\omega_2 L_{mr} I_{s2} \sin \delta)^2 / R_{mr}. \quad (17)$$

Where  $I_{r1}$  is the rotor current component due component due to rotor fed as indicated by eqs. (3) and (5), respectively. The stator and rotor power factors,  $\cos \phi_s$  and  $\cos \phi_r$  are determined from eqs. (9, 10), respectively. Therefore, the motor efficiency  $\eta$  can be determined.

## 5. System characteristics

### 5.1. Load angle and machine characteristics

Considering the net air gap MMF in terms of equivalent current as  $I\phi$ , the angle between  $I\phi$  and the stator current  $I_1$  is  $\alpha_1$  and between the rotor current  $I_2$  and  $I\phi$  is  $\alpha_2$ . Taking  $\delta$  as the load angle between the two magnetic axes (stator and rotor MMF axis), Then,  $\delta = \alpha_1 + \alpha_2$ . In the case of dc excited synchronous machine  $\alpha_2 = \pi/2$ , the load angle  $\delta = \alpha_1 + (\pi/2)$ . The machine operates with either advanced rotor (+ve load angle) or with retarded rotor (-ve load angle). Using the proposed machine analysis given in section 4, the machine characteristics are computed and presented as shown in figs. 4 to 17. The resultant synchronous torque in each case may be either motoring or generating torque depending on the load angle value and the machine parameters as shown in fig. 4. Operation with retarded rotor results in self starting and greatly improves the efficiency and increases the overloading capability as shown in figs. 4 and 8.

### 5.2. Motor performance characteristics

The proposed axial motor performance is computed using the axial motor parameters

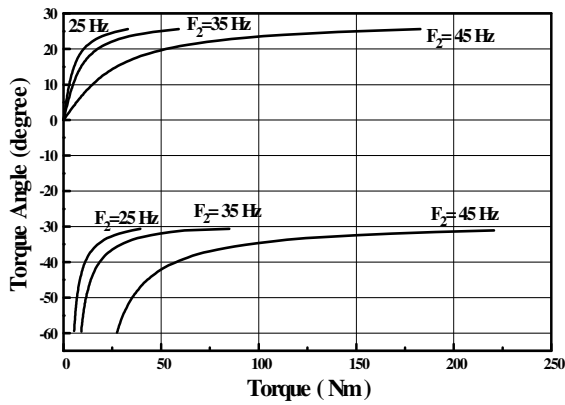


Fig. 4. Motor torque as affected by Load angle variation at different frequencies.

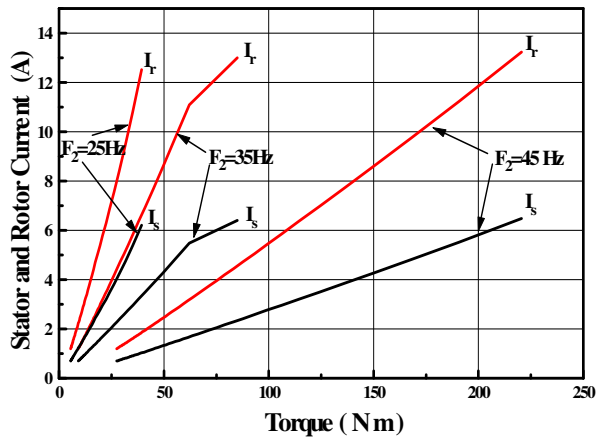


Fig. 5. Stator and rotor current variation versus load torque.

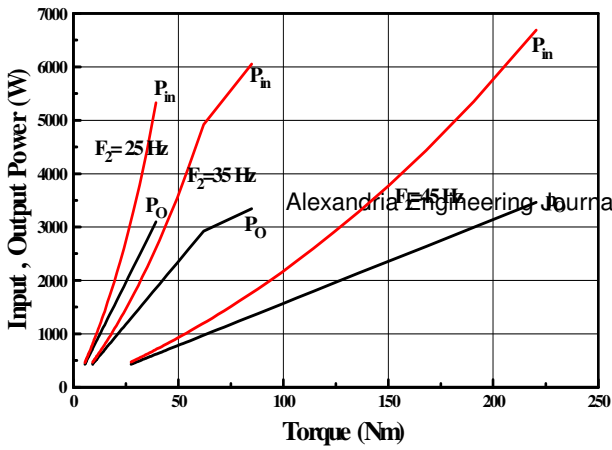


Fig.6. Input and output power variation versus load torque.

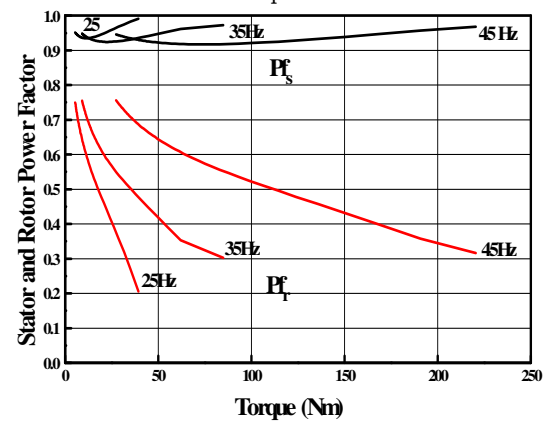
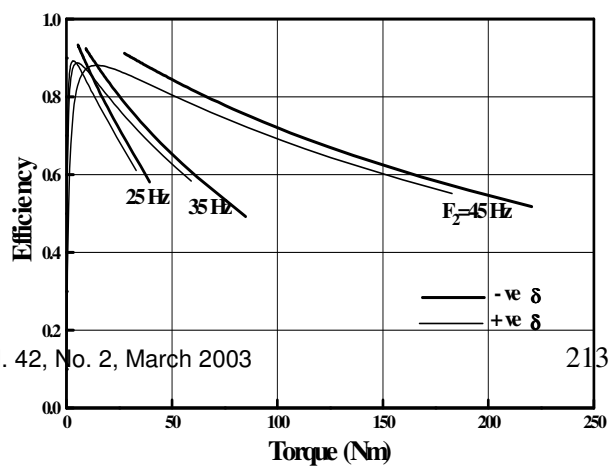


Fig.7. Stator and rotor power factor versus load torque.



### 5.3. Motor performance for EV

It is superior to show that the proposed motor handles the desired EV optimum torque- speed profile in both speed directions as shown in fig. 9. In this technique the maximum motoring speed is its base speed (1500 rpm) and control is achieved to operate the motor entirely in constant power region. Constant power is achieved from near zero speed up to maximum speed for motoring operation in both forward and backward speed operating modes as shown in fig. 10. Stator and rotor currents maintain their constancy over the maximum motoring speed and increases rapidly at speeds close to base speed (maximum speed range as shown in fig. 11. Thus the motor is capable of short term over loading due to the good ventilation at high speeds. Fig. 12 shows the high efficiency which increases significantly as the constant power – speed range increases. High stator power factor and acceptable rotor power factor are obtained as shown in fig. 13.

Fig . 8. Efficiency as affected by load angle variation.

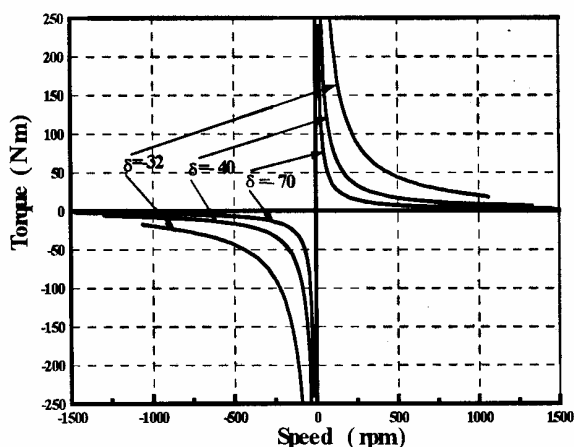


Fig.9. AFSM Optimum torque / speed profile as required for EV & HEV.

given in table 1. Figs. 5, 6,7 and 8 represent these performances at different excitation frequencies from no load up to full load. These figures show the relation between motor currents (stator and rotor), input power, output power and power factor (stator & rotor) versus motor torque at different frequencies, At high exciting frequency of 45 Hz (150 rpm), the motor can be loaded with much higher torque than its full load (fig. 5 ) as both stator and rotor currents increase slowly. As the rotor frequency decreases (speed increases) the motor torque decreases significantly. Fig. 6 shows the output and input power variation. The efficiency increases remarkably at the relatively reduced loads as shown in fig. 8.

### 6. Experimental test RIG

To verify the validity of the theory and analysis of the proposed motor as well as the effectiveness of the proposed strategy, an experimental system is implemented. Because of the difficulty of building an axial flux motor in our laboratory, two identical wound rotor induction motors (radial flux) have been

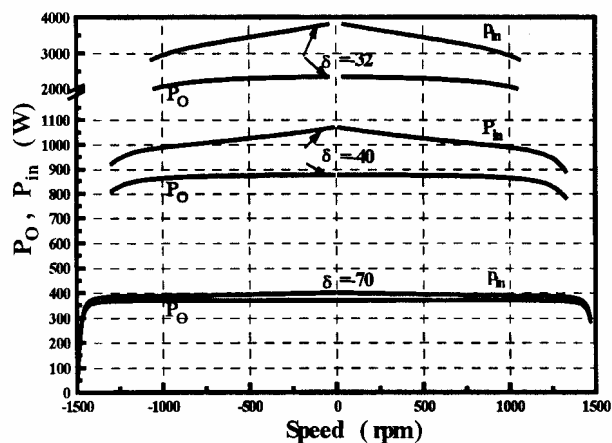


Fig. 10. Input and output power / speed.

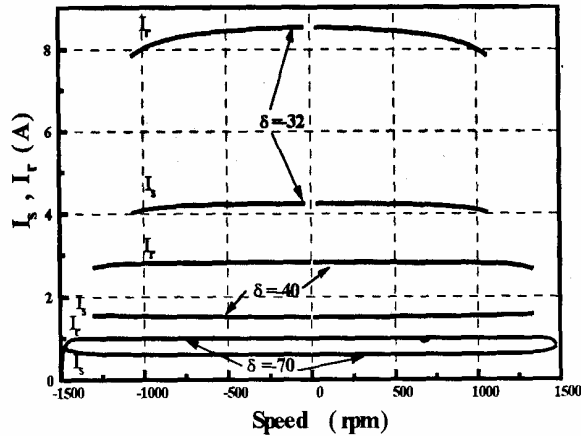


Fig. 11. Stator and rotor current / speed.

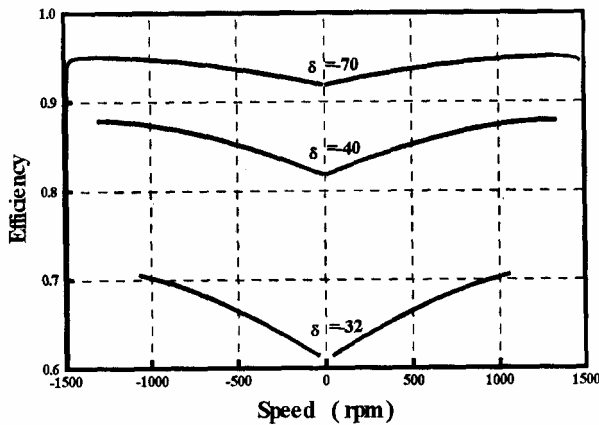
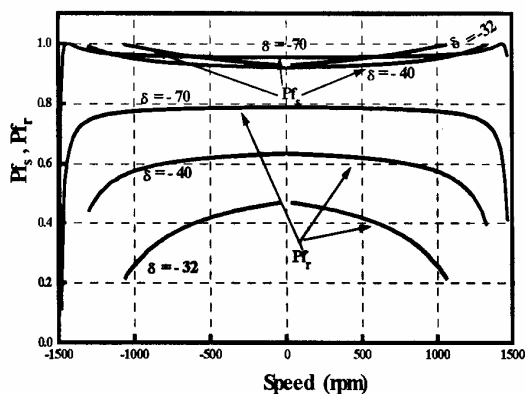


Fig. 12. Efficiency versus speed.



urnal, Vol

Fig. 13. Stator and rotor power factor/speed.

chosen (having the same power and pole numbers of the proposed axial motor) to simulate the proposed motor. The two stator windings are connected together in series with same polarity while the two rotor windings are connected together in reverse series. The two motor shafts are mechanically coupled in selsyn mode and loaded by a dc dynamometer. The stator is fed from 50 Hz supply while the rotor was fed from a frequency converter. Experimental results are shown in figs. 14-17. In the same figures, the corresponding computed characteristics using the parameters of radial flux motor (used for experimental work) and that of axial flux motor (modified due to the basis stated in refs. [13, 14]) are illustrated for comparison. The differences between axial flux and radial flux performance are as expected based on the comparison given in the above mentioned references and described in section 2-2. The machine performance is sensitive to load angle variation. Thus the deviation between the theoretical characteristics and experimental ones are acceptable. Both axial flux and radial flux motor data are listed in table 1.

### 7. Conclusions

A new three phase – 4 pole self-started ac excited – axial flux synchronous motor of twin stator-single rotor has been proposed. In addition to axial flux machine advantages, the proposed motor may be considered as an optimum drive for electric vehicle. Its advantages lie on;

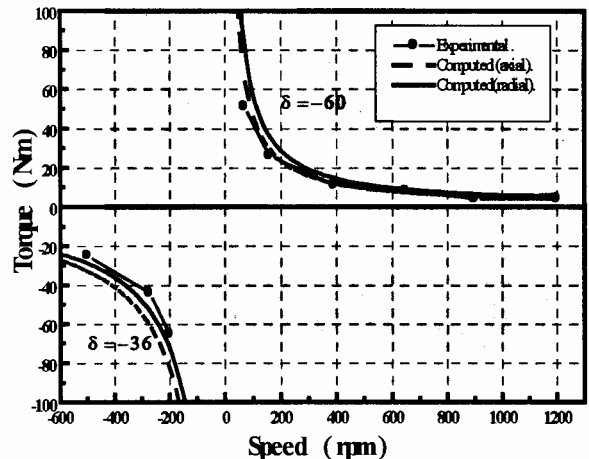


Fig.14. Experimental torque / speed characteristics.

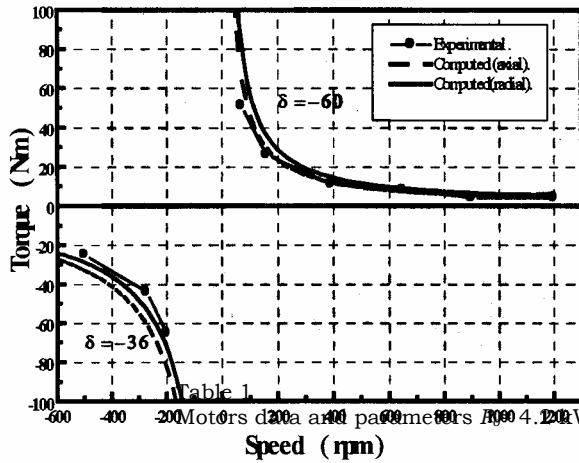


Fig. 15. Experimental current / speed characteristics.

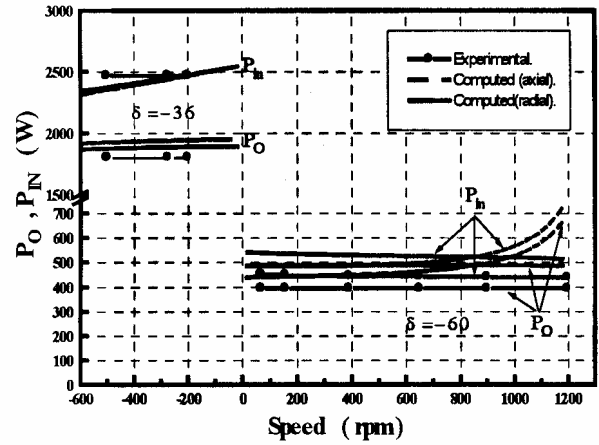


Fig.16. Experimental power / speed.

Motors data and parameters are given in Table 1.  $P_{ph} = 220 \text{ W}$ ,  $V_{ph} = 220 \text{ V}$ ,  $f = 50 \text{ Hz}$ ,  $N_s = 1500 \text{ rpm}$

Data and parameters	Unit	Radial flux motor	Axial flux motor
Number of poles	-	4	4
Stator phase current	A	8	8
Stator phase resistance	$\Omega$	2.22	2.01
Stator phase leakage reactance	$\Omega$	5	2.646
Rotor phase resistance	$\Omega$	1.52	1.38
Rotor phase leakage reactance	$\Omega$	2.45	1.29
Magnetizing reactance	$\Omega$	166.17	196.3

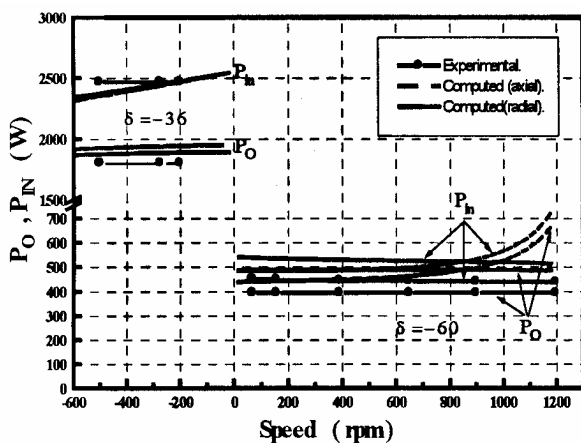


Fig. 17. Experimental efficiency / speed.

1. It yields the optimum torque – speed profile required for EV.
2. Inverter KVA and motor power requirements are minimum due to operating the motor entirely in the constant power range.
3. Very wide constant power region.
4. High efficiency and power factor due to operation at and below base speed.
5. Low cost.
6. Short term over loading capability.
7. Direct coupling without reduction gear box.

The simulation and experimental results verified the effectiveness of the new approach for high performance AC excited – axial flux



synchronous motor for electric vehicle drive.

### References

- [1] R. M. Khwaja and E. Mehrdad, "Design Consideration for EV and HEV motor Drives " Proc. ICEM Conf., pp. 2065-2070 (1998).
- [2] Rahman, "A Permanent Magnet Hysteresis Hybrid Synchronous Motor for Electric Vehicles" IEEE Transactions on industrial Electronics, Vol. 44 (1), pp. 46-53 (1997).
- [3] A. Massash and K. Shinnichiro, "Overview of Recent Development of EVs and HEVs in Japan" Proc. IPEC – Tokyo, pp. 1960-1966 (2000).
- [4] A. Lange and W.R. Canders, F. Laube, H. Mosebach "Comparison of Different Drive Systems for a 75 KW Electrical Vehicle Drive" Proc. ICEM, Finland, pp. 1308-1312 (2000).
- [5] A. Benoudjit and S. Nait, "Effects of Design parameters Choice on the Performances OF axial & radial flux induction Motors for on wheel Drive" Proc. 34th UPEC Conf. Leicester, UK., pp. 267-270 (1999).
- [6] G. Cvetkovski and S. Gair, " Quasi 3D FEM in Function of an Optimization Analysis of a PM Disc Motor" Proc. ICEM, Espoo – Finland, pp. 1871-1875 (2000).
- [7] Z. Szymanski "Adaptive Mode Control System in Electric Drive System of the Hybrid Wheel Vehicles" Proc. ACEMP, pp. 83-88 (2001).
- [8] R. E. Colyer, "Electric Drives in military Vehicles" Proc. ACEMP, Turkey, pp. 73-78 (2001).
- [9] M. Ehsani and M. Khwaja, T. Hamid, "Propulsion system Design of Electric and Hybrid Vehicles" IEEE Trans. on Indus. Electronics, Vol. 44 (1), pp. 19-27 (1997).
- [10] S. Sasha and S.Verma "Analytical Development and Computer Simulation of an Electric Vehicle" Proc. ICEM, Finland, pp. 553-557 (2000).
- [11] F. Profumo and A. Tenconi, Zhangz, A. Cavagnino " Design and Realization of a novel Axial Flux Interior PM synchronous Motor For Wheel Motors Applications" Proc. ICEM, pp.1791-1796 (1998).
- [12] Wiaks "Disc Type Motors For Light Electric vehicles" Proc. ACEMP, Turkey, pp. 447-452 (2001).

- [13] F. Profumo and Z. Zheng , T. Alberto  
“Axial Flux Machines Drives: A New  
viable Solution For Electric Cars” IEEE  
Trans. on Indus. Electronics, Vol. 44, pp.  
39-45 (1997).
- [14] D. Platt and B. Smith “Twin rotor Drive  
for an electric Vehicle” IEE Proc., B, Vol.  
140 (2), pp. 131-138 (1993).

Received November 16, 2002

Accepted March 27, 2003